Perception, 1996, volume 25, pages 543–567

Cortical dynamics of boundary segmentation and reset: persistence, afterimages, and residual traces

Gregory Francis
Department of Psychological Sciences, Purdue University, 1364 Psychological Sciences Building, West Lafayette, IN 47907, USA

Stephen Grossberg¶
Center for Adaptive Systems and Department of Cognitive and Neural Systems, Boston University, 677 Beacon Street, Boston, MA 02215, USA
Received 24 January 1995, in revised form 24 July 1995

Abstract. In previous work with a neural-network model of boundary segmentation and reset, the percept of persistence was linked to the duration of a boundary segmentation after stimulus offset. In particular, the model simulated the decrease of persistence duration with an increase in stimulus duration and luminance. Further evidence is revealed for the neural mechanisms involved in the theory. Simulations show that the model reset signals generate orientational afterimages, such as the MacKay effect, when the reset signals can be grouped by a subsequent boundary segmentation that generates illusory contours through them. Simulations also show that the same mechanisms explain properties of residual traces, which increase in duration with stimulus duration and luminance. The model hereby discloses previously unsuspected mechanistic links between data about persistence and afterimages, and helps to clarify the sometimes controversial issues surrounding distinctions between persistence, residual traces, and afterimages.

1 Introduction

Grossberg (1991) qualitatively analyzed a neural model of emergent boundary segmentation, called the Boundary Contour System (BCS), and noted that the positive feedback in the model, which helps to select correct groupings and maintain their coherence, could also cause smearing in respect to changing images. In this analysis a mechanism to reset the positive feedback was identified and it was noted how reset signals generated at stimulus offset could control smearing. Francis et al (1994) quantitatively simulated the BCS model and showed that a key process governing the persistence of visual percepts is the time taken to reset a segmentation. This analysis explained characteristics of illusory-contour persistence (Meyer and Ming 1988), effects of orientation-specific adaptation (Meyer et al 1975), spatial masking (Farrell et al 1990), and inverse relationships between persistence and stimulus luminance and duration (Bowen et al 1974). Francis (1996a) simulated the model to explain relationships between persistence and interstimulus intervals of masking stimuli (Castet 1994). Francis and Grossberg (1996) further developed the model to show how persistence influences percepts of apparent motion, including interattribute apparent motion (Cavanagh et al 1989; von Grünau 1979) and Korte's Laws (Kolers 1972; Korte 1915; Neuhaus 1930).

In the current work we suggest that the reset signals necessary to prevent smearing of segmentations, which were described in Francis et al (1994), can create afterimage percepts. We identify two sets of psychophysical data that match the properties of these reset signals. The first data set identifies orientational afterimages. The second data set identifies residual traces, which are sometimes found in studies of visual persistence. We argue that both effects arise out of a need to reset resonating segmentations in a neural network for boundary segmentation. In addition, we explain why in many

¶ Author to whom requests for reprints should be addressed.

persistence studies researchers fail to find evidence of residual traces. Our analysis hereby sheds some light on why the relationship between persistence per se and the residual effects which sometimes occur in a persistence paradigm have been so controversial. In the next section we discuss the data in more detail.

1.1 *Orientational afterimages*

MacKay (1957) reported an orientational afterimage after viewing a set of concentric outline circles for several seconds and then looking at a blank screen. The afterimage consists of a perceived radial form (figure 1). Similarly, viewing a set of radial lines, passing through a common center point, produces a circularly organized afterimage.

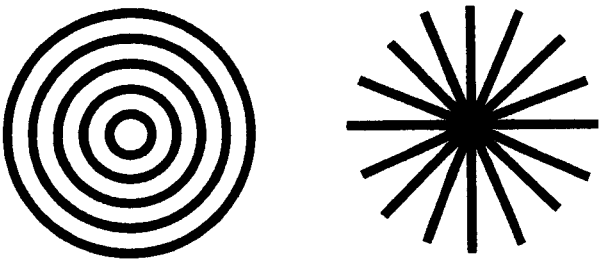

Figure 1. Prolonged fixation followed by offset of a set of concentric circles produces an afterimage with a radial organization.

1.2 *Residual traces*

A common problem for psychophysical studies of dynamic vision is to avoid retinal afterimages. If subjects can perform a task by taking advantage of retinal afterimages, the task will not permit measurement of the duration of persisting representations of the original percept. This is important for studies of visual persistence because the duration of retinal afterimages is known to increase with stimulus luminance and duration (Brown 1965). In contrast, many studies of visual persistence in which retinal afterimages are not produced show that persistence decreases with stimulus luminance and duration [see the review on luminance effects by DiLollo and Bischof (1995)].

It is important to distinguish between studies in which retinal images are probably produced and those in which they are not because there has been a heated debate among researchers of persistence about whether persistence duration increases or decreases with stimulus luminance and duration. Long and his colleagues (eg Long 1980) argued (following Hawkins and Shulman 1979) that there exist two types of persistence signals. Type-1 signals were claimed to be inversely related to stimulus luminance and duration, whereas type-2 signals were claimed to be directly related to the same variables. In a series of experiments involving probe displays, Long and colleagues tried to explore the properties of type-2 signals. However, those efforts have been strongly criticized (DiLollo 1984; DiLollo and Bischof 1995; DiLollo et al 1988; Irwin and Yeomans 1986a) because it is likely that subjects' results were based upon retinal afterimages, rather than persistence of the original percept. Such criticism appears justified, as many of the studies involved very intense stimuli, dark-adapted subjects, or both.

On the other hand, there are a few studies that were unlikely to involve retinal afterimages but still reveal increases in persistence with increases in stimulus luminance and/or duration (Long and McCarthy 1982; Long and Sakitt 1981; Long and Wurst 1984). In the study by Long and McCarthy, subjects participated in two different versions of an experiment. By means of probe-asynchrony measures (reaction-time measures produced similar results), subjects first judged the perceived offset of

the visual image. For these judgments, the data (replotted in figure 2a) show inverse effects between persistence and stimulus duration and luminance.

In a second test, the same subjects judged the disappearance of any perceived residual trace. For these judgments the data (replotted in figure 2b) show a direct effect of stimulus duration and luminance on duration of residual traces. Long and McCarthy (1982) argue that residual traces provide a more complete description of the properties of visual persistence.

Critics of these experiments (DiLollo 1984; DiLollo and Bischof 1995; Irwin and Yeomans 1986a) argued that the probe-matching and reaction-time measures are unreliable and cannot be trusted for drawing conclusions about persistence. Such caution is to be commended, given that direct relationships between persistence and stimulus luminance and duration appear only with certain measures and then only under certain conditions. Other measures of persistence, such as form-integration studies,

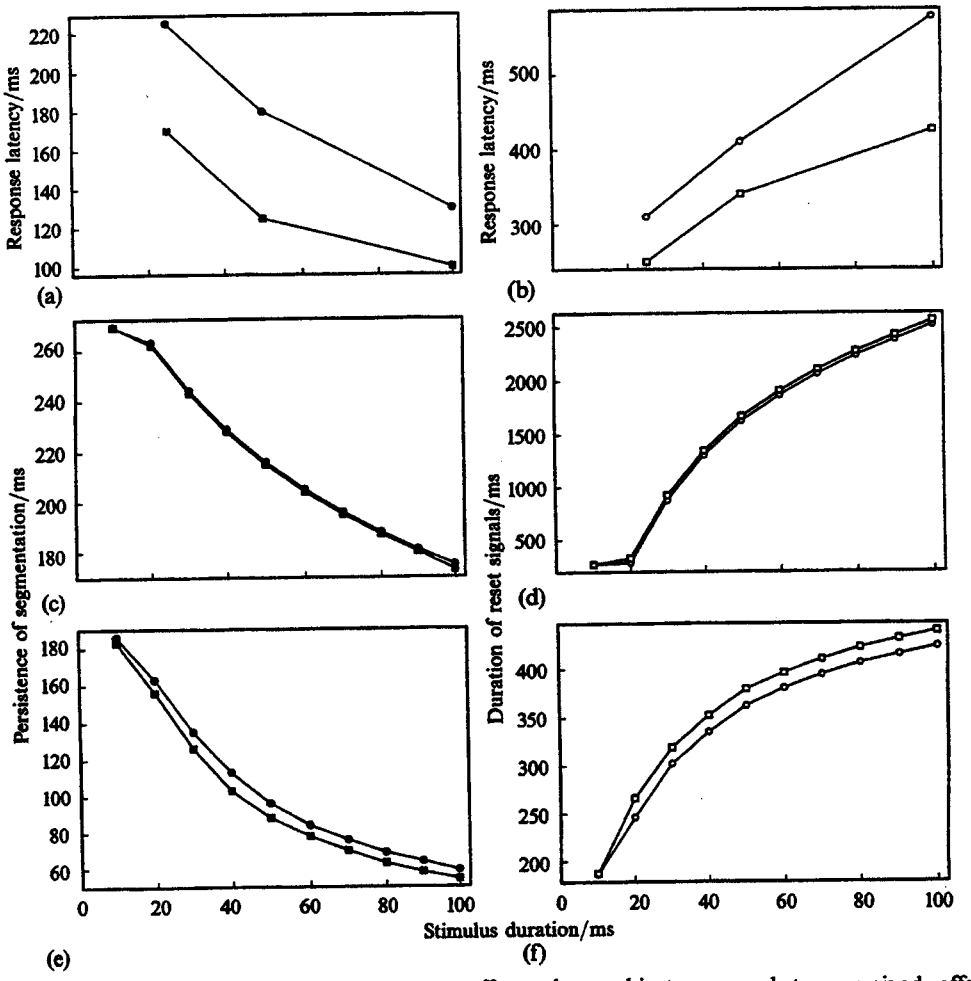

Figure 2. (a) Response latency to target offset when subjects respond to perceived offset. (b) Response latency to target offset when subjects respond to any residual trace of the target. Data in (a) and (b) are replotted with permission from Long and McCarthy (1982). (c) Simulation results for the persistence of segmentation signals. (d) Simulation results for the duration of reset signals. (e) and (f) The same qualitative characteristics exist in model simulations with a different set of parameters. Circles are data for 5.0 ft L and squares for 15.0 ft L. (Note: 1 ft L = 3.43 cd m^{-2}.)

reveal no evidence of residual traces, even though it appears such traces would help subjects perform their experimental task. Thus, direct relationships must be regarded as secondary to the properties of persistence and should be distinguished from the persisting percept measured with other techniques.

However, to argue that a set of data cannot be directly compared with other sets of data does not explain the original data. Even though the residual traces measured by Long and McCarthy (1982) cannot be considered as measures of persisting percepts, they remain properties of dynamic vision that models of visual perception need to explain. Indeed, the ability to explain data on the fringes of a research domain provides strong support for a model that can also explain the main effects.

We agree with the above critics that the properties of residual traces found by Long and McCarthy (1982) should not be taken as properties of visual persistence per se. We suggest that residual traces are more properly viewed as a type of cortical afterimage. Moreover, we suggest that residual traces have a close relationship to persistence data, not as signals responsible for persistence, but as correlated signals that help to shorten persisting signals. This close relationship cannot easily be understood or even described without a model that summarizes the temporal unfolding of the underlying visual process. In section 2 we describe such a model and its dynamic properties.

The simulations reported in this article involve the identical equations and parameters that were used in Francis et al (1994) to simulate data about persistence and in Francis and Grossberg (1996) to simulate data about form–motion interactions. Our goal in all these studies is to show that the same model mechanisms qualitatively reproduce all of these data, without a change of parameters, in order to support our conceptual arguments about the meaning of these data. We also display results of additional simulations with different parameters to demonstrate the robustness of the qualitative effects and the fact that quantitative fits are possible within the model. A more extensive parameter search for quantitative data fits is premature both because the subject responses are quite variable and the model has been significantly simplified to make it computationally tractable in response to changing imagery.

2 Boundary segmentation and surface representation

2.1 *Boundary segmentation by the BCS*

Grossberg (1984) and Cohen and Grossberg (1984) introduced the Static-BCS model. Grossberg and Mingolla (1985a, 1985b, 1987) developed the model to simulate how the visual system detects, completes, and regularizes boundary segmentations in response to a variety of retinal images. Such segmentations can be defined by regions of different luminance, color, texture, shading, or stereo signals. The Static-BCS computations for single-scale monocular processing consist of a series of filtering, competitive, and cooperative stages as schematized in figure 3 and reviewed in several reports (eg Grossberg 1987a, 1994; Grossberg et al 1989). The first stage, schematized as an unoriented annulus in figure 3, models in perhaps the simplest possible way the shunting on-center off-surround interactions at the retinal and LGN levels. These interactions compensate for variable illumination, enhance regions of local contrast in the image, compute Weber-law-modulated ratio contrasts at regions of local contrast, and normalize cell activities (Grossberg 1983). Interactions of on-center off-surround ON cells and off-center on-surround OFF cells are not needed here, but their complementary responses to images are modeled elsewhere (Gove et al 1994, 1995; Grossberg and Wyse 1991; Grossberg et al 1994; Pessoa et al 1995).

These model LGN cells input to pairs of like-oriented simple cells that are sensitive to opposite contrast polarity, or direction of contrast. The simple-cell pairs, in turn, send half-wave-rectified output signals to like-oriented complex cells. Complex cells

hereby pool signals from simple cells that are sensitive to opposite contrast polarities. These opposite-polarity half-wave-rectified signals combine in such a way that complex cells compute a full-wave-rectified measure of oriented image contrast. In this sense, complex cells are rendered insensitive to direction of contrast, as are all subsequent cell types in the model.

Complex cells activate hypercomplex cells through an on-center off-surround network (first competitive stage) whose off-surround carries out an end-stopping operation. In this way, complex cells excite hypercomplex cells of the same orientation and position, while inhibiting hypercomplex cells of the same orientation at nearby positions. One role of this spatial competition is to spatially sharpen the neural responses to oriented luminance edges, especially at line ends. Another role is to initiate the process, called end cutting, whereby boundaries are formed that abut a line end at orientations perpendicular or oblique to the orientation of the line itself (Grossberg 1987a; Grossberg and Mingolla 1985b).

The signals from complex cells to hypercomplex cells are multiplied, or gated, by habituative chemical transmitters. These habituative gates help to reset boundary segmentations in response to rapidly changing imagery, as discussed below. The hypercomplex cells input to a competition across orientations at each position (second competitive stage) among higher-order hypercomplex cells. This competition acts to sharpen up orientational responses at each position, and to work with the habituative gates to reset boundary segmentations, as discussed below.

Output from the higher-order hypercomplex cells feed into cooperative bipole cells that initiate long-range boundary grouping and completion. Bipole cells fire only if both of their receptive fields are sufficiently activated by appropriately oriented hypercomplex-cell inputs. Bipole cells hereby realize a type of long-range cooperation among the outputs of active hypercomplex cells. For example, a horizontal bipole cell, as in figure 3, is excited by activation of horizontal hypercomplex cells that input to its horizontally oriented receptive fields. A horizontal bipole cell is also inhibited by activation of vertical hypercomplex cells.

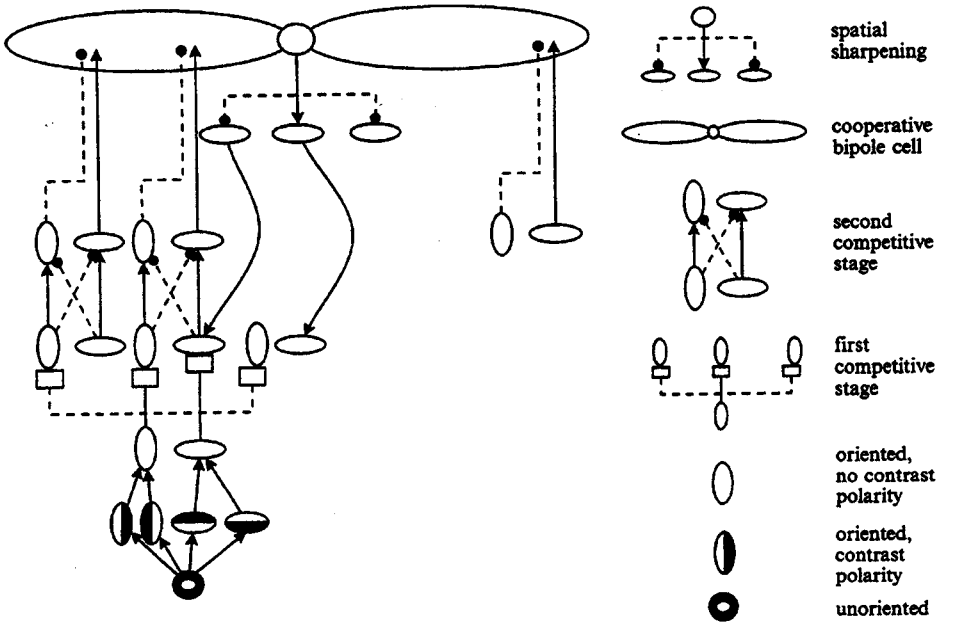

Figure 3. Boundary Contour System with embedded gated dipoles.

Bipole cells were predicted to exist in Cohen and Grossberg (1984) and Grossberg (1984) shortly before cortical cells in area V2 with similar properties were reported by von der Heydt et al (1984). At around the time of the von der Heydt et al report, Grossberg and Mingolla (1985a, 1985b) used bipole-cell properties to simulate and explain a variety of data about illusory-contour formation, neon color spreading, and texture segregation. These same properties play a role in our explanations of apparent motion of illusory contours and interattribute apparent motion (Francis and Grossberg 1996).

Bipole cells generate feedback signals to like-oriented hypercomplex cells. These feedback signals help to create and enhance spatially and orientationally consistent boundary groupings, while inhibiting inconsistent ones. In particular, bipole-cell feedback excites hypercomplex cells at the same orientation and position while inhibiting cells at nearby positions. Hypercomplex boundary signals with the most cooperative support from bipole grouping thereupon further excite the corresponding bipole cells. This cycle of bottom–up and top–down interaction between hypercomplex cells and bipole cells rapidly converges to a final boundary segmentation. Feedback among bipole cells and hypercomplex cells hereby drives a resonant cooperative–competitive decision process that completes the statistically most-favored boundaries, suppresses less-favored boundaries, and coherently binds together appropriate feature combinations in the image.

2.2 *Surface representation by the Feature Contour System*

The boundary segmentation of the BCS works with a complementary surface-representation system called the Feature Contour System (FCS). Because BCS output signals pool opposite contrast polarities, they do not carry a perceptually visible signal. They gain visibility by interacting with the FCS. BCS output signals to the FCS define region boundaries. Signals from the model LGN activate a diffusion process within the FCS which fills in surface properties like brightness, color, and depth within these boundaries.

Figure 4 summarizes some key steps in the process whereby BCS signals 'capture' or bind FCS signals for filling in of surface representations. This binding process is illustrated through an analysis of percepts of binocular rivalry (Grossberg 1987b). The FCS consists of separate monocular retinal and LGN pathways corresponding to inputs from the right or left eye. In figure 4, the right eye receives stimulation from a horizontally oriented grating, while the left eye receives stimulation from a vertically oriented grating. Under such conditions, subjects report seeing either a vertical grating or a horizontal grating, but they do not see both at the same time in the same location (Kaufman 1974).

The FCS contains opponent and double-opponent ON-cell and OFF-cell stages that respond to spatial changes in luminance and color. These are indicated by the on-center off-surround receptive field at the side of each such schematized stage. The FCS also contains filling-in domains where these center–surround responses diffuse within regions defined by the spatial organization of boundary signals from the BCS. Cross-shaped structures of cells mark these stages, indicating that the activity of the center cell diffuses to the surrounding cells, and vice versa. The presence of a boundary signal restricts this diffusion process. As a result, a set of boundary signals can contain the diffusion of FCS signals, and prevent it from spilling into regions outside the boundary signals.

Input from each eye contributes to the creation of BCS boundary signals. These BCS boundaries attempt to fuse signals from both eyes to generate a boundary representation that is sensitive to the relative depths of objects from the observer. In response to left-eye and right-eye inputs that are mutually perpendicular, fusion cannot occur.

Instead, binocular rivalry is initiated by the orientational competition (second competitive stage, figure 3) among the hypercomplex cells. When the winning hypercomplex cells interact with the cooperative bipole cells, they generate a boundary segmentation within each region that favors the horizontal grating or the vertical grating at any location and time, and suppresses the other one.

Grossberg (1987b, 1994) modeled how this selection takes place and how rivalrous percepts emerge through time. For present purposes, suppose that the BCS generates boundaries consistent with the horizontal grating of the right eye. These BCS boundaries interact with each monocular pathway of the FCS at the first filling-in stage. For the right-eye pathway, the spatial organization of the binocular boundary signals and the monocular FCS signals are similar. The filling-in domains are designed so that filling in is activated when the BCS and FCS signals are spatially aligned in this way. As a result, a visible-surface representation of horizontal bars fills in only within the filling-in domain whose relative depth corresponds to that of the active BCS boundaries. The left-eye pathway produces a different result. Here, the FCS monocular signals are spatially organized into vertical bars, but the binocular BCS signals are spatially organized as horizontal bars. As a result, at the filling-in stage of the left-eye pathway, the FCS signals diffuse throughout the stage, both inside and outside the regions delineated by the BCS signals.

The difference between the filling-in events corresponding to the right and left eyes produces dramatically different responses at the next FCS stage of each pathway. For the right-eye pathway, the on-center off-surround cells of the next stage respond to contrast boundaries of the filled-in activities. The resulting responses look similar to the responses produced at the first on-center off-surround stage in the right-eye pathway. The BCS signals hereby capture FCS data of the horizontal grating for

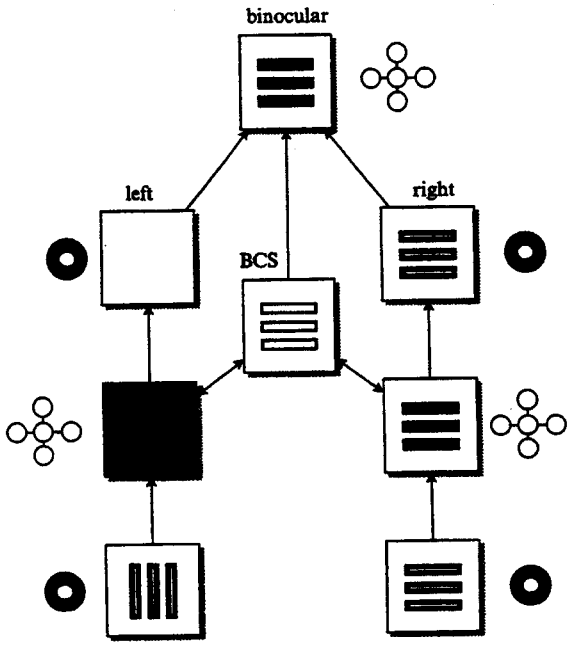

Figure 4. Binding or capture of FCS signals by BCS signals. Each monocular pathway of the FCS contains stages of on-center off-surround interactions, which detect spatial changes in activity, and filling-in domains where activities diffuse across regions defined by BCS signals. The resulting interactions force the filled-in binocular surface representation to correspond to the organization of the boundary signals. See text for details.

subsequent processing. The responses to the filled-in activities of the left-eye pathway are quite different. Here the activities in the filling-in stage of the left-eye pathway have spread out to cover the entire spatial extent of the image. The on-center off-surround and opponent interactions between ON and OFF cells inhibit all outputs. The BCS signals hereby delete FCS data of the vertical grating from subsequent processing.

Both the left-eye and the right-eye pathways feed into a binocular stage of filling in at which perceived surface brightness is represented. Here, the binocular boundary signals again define the regions that contain the diffusion of FCS signals. Since the left-eye FCS pathway does not register the vertical inputs of the left eye, the resulting spatial organization of activities at the binocular filling-in stage looks like a horizontal grating at the appropriate relative depth from the observer. The FCS activities in the left-eye pathway make no contribution to the binocular percept even though they generate large inputs to the first stages of model cortical processing.

At times when the BCS generates vertical boundaries that are consistent with the grating presented to the left eye, then the same BCS–FCS interactions pick out the FCS responses to the vertical grating and suppress the responses to the horizontal grating. Thus, the boundary signals of the BCS are capable of selectively capturing the FCS signals to produce a surface percept of form and color and depth, or FACADE. As is shown below, the ability of the BCS to capture or bind FCS signals controls the persistence of perceived brightness.

2.3 *The dynamics of boundary and surface reset*

The positive feedback within the hypercomplex–bipole feedback loop of the BCS is critical for selecting sharp boundary groupings and inhibiting weaker ones, but it also creates hysteresis that could, if left unchecked, lead to undesirably long boundary persistence after stimulus offset, and thus to uncontrolled image smearing in response to image motion. In particular, each cell in the BCS has its own local

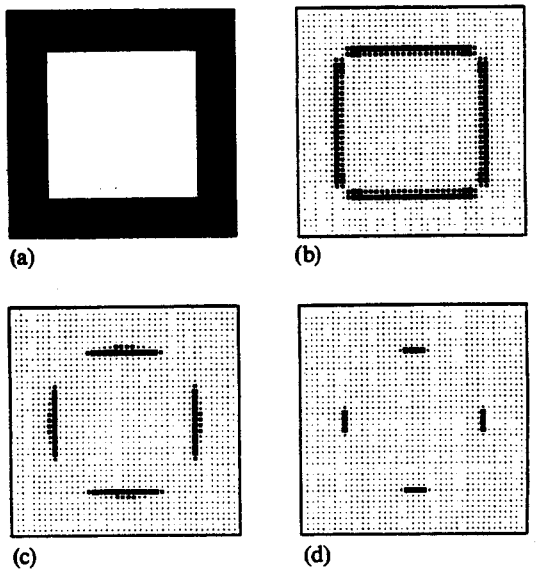

Figure 5. A demonstration of boundary erosion. Solid squares indicate positive activity of level 6 boundary cells (see the appendix). The smaller dots mark pixel locations. (a) Stimulus input to the network, a bright square on a dark background. (b) Boundary response to the square shortly after the input returns to the background level. (c) Boundary signals start to erode from the corners of the square toward the middle of the contours. (d) Boundary erosion is almost complete. Reprinted from Francis et al (1994) with permission.

dynamics involving activation by inputs and passive decay (of the order of 10 simulated ms). However, the excitatory feedback loop dominates the temporal aspects of the BCS. As shown in Francis et al (1994), when inputs (luminance edges or illusory-contour inducers) feed into the BCS, they trigger reverberatory interactions that, if left unchecked, can last for hundreds of simulated milliseconds.

This is true because activities of hypercomplex and bipole cells at a particular position and orientation decay away only when bipole-cell output centered at the same position and orientation weakens. Since bipole-cell activation depends on inputs to both receptive fields, bipole activation near the ends of contours weakens first after inputs shut off. As these bipole cells lose activation, so do all other cells of the same orientation and position. This decay causes activities of more bipole cells to decay, which continues the process. The net effect of these spatial and temporal interactions is that boundary activities erode from contour ends to the contour middle (see Francis et al 1994). McFarland (1965) has reported analogous data.

Figure 5 summarizes a simulation of boundary-signal erosion. Figure 5a shows the stimulus presented to the system, a bright square on a dark background. Figures 5b–5d show the boundary-signal response to the luminance edges of the stimulus at successive moments beyond stimulus offset. The figures show the erosion of boundary signals from the corners of the stimulus to the middles of the contours.

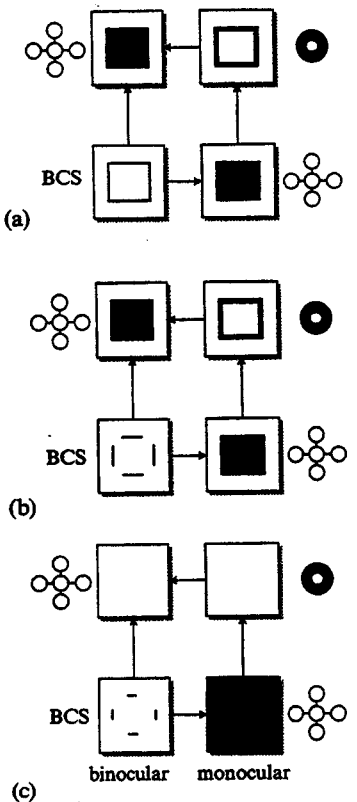

Figure 6. Schematic diagram of how the dynamics of the binding process after stimulus offset control visual persistence. (a) When boundaries are strong and bind FCS activities, the binocular FCS activities are strong. (b) As boundaries erode, they less effectively bind FCS activities, and so the binocular FCS activities weaken. (c) As boundaries erode further, they cannot bind FCS activities at all, so the binocular FCS activities disappear. Disappearance of binocular FCS activities corresponds to perceived offset of the stimulus.

Figure 6 summarizes how the erosion of boundaries at stimulus offset results in an unbinding of monocular FCS signals and the disappearance of a binocular brightness percept. Figure 6a schematizes the system response just after stimulus offset, as in figure 5b. The boundaries continue to bind FCS activities, and to produce a response in the binocular FCS filling-in domain. Figure 6b schematizes the system response after BCS boundaries have eroded somewhat, as in figure 5c. Here, the boundaries bind some FCS activities and produce a binocular FCS response, although not as strong or as sharply delineated as before. Figure 6c schematizes the system response at a still-later point in time, when the boundary erosion is almost complete, as in figure 5d. Here, the boundaries cannot bind any FCS activities and thus there is no binocular FCS response.

Since the activities of the binocular FCS filling-in domain correspond to a subject's perception of stimulus brightness, the time of disappearance of these activities corresponds to the offset of the stimulus brightness. The time between physical offset of the stimulus and the disappearance of FCS activities corresponds to measures of visual persistence of the brightness percept. The dynamical nature of binding by the BCS controls the disappearance of the binocular FCS activities. The rate of erosion among the boundary signals controls the dynamics of the binding process. Thus, visual persistence correlates with the erosion of the boundary signals. In particular, when the boundaries of an edge erode to such a degree that they no longer bind FCS monocular activities, then the binocular FCS activities disappear. Thus, visual persistence is related to the duration of BCS signals. This measure was used by Francis et al (1994) and Francis (1996a) to explain properties of visual persistence.

2.4 *Reset signals and gated dipoles*

As noted above, systems with visual persistence need to avoid image smearing. The problem for the BCS is to accelerate the boundary erosion and unbinding of feature signals in response to rapidly changing imagery. More generally, the BCS needs to use resonant feedback to maintain segmentations of unmoving scenic objects, even as it actively resets segmentations corresponding to rapidly changing scenic objects. The net effect is to control image smearing in a form-sensitive way. Remarkably, the same BCS mechanisms that create resonant boundaries also reset them. Two types of mechanisms maintain the desired trade-off between resonance and reset. One mechanism is the lateral inhibition that converts complex cells into hypercomplex cells via end-stopping (first competitive stage, figure 3). Its role is described in Francis et al (1994) and Francis (1995, 1996a, 1996b). The other mechanism will be the focus of this article. It uses the orientational competition that converts model hypercomplex cells into higher-order hypercomplex cells. Consider how this competition works between pairs of mutually perpendicular cells. Pairs of mutually perpendicular complex, hypercomplex, and higher-order hypercomplex cells define a specialized type of opponent-processing circuit that Grossberg (1972) has called a gated dipole. The gates in the dipole are habituative transmitters that multiply signals in the pathways from complex to hypercomplex cells (square synapses in figure 3). Such a gated dipole can rapidly inhibit a bipole cell when its activating image features shut off or are removed owing to image motion.

To understand better how this works, see figure 7, which shows a subset of the cells from figure 3 consisting of separate pathways sensitive to the same position in visual space but having perpendicular orientations. These pathways compete through the second competitive stage of hypercomplex cells. Feeding this competition are inputs gated by habituative transmitters. Along with signals from external stimuli, each input pathway receives a tonic source of activity, and all output signals are rectified. It is this combination of rectification, opponent competition, habituative-transmitter gates, and tonic input that, in a variety of specialized circuits, constitutes a gated dipole.

At the offset of stimulation, a gated-dipole circuit generates a transient rebound of activity in the previously nonstimulated pathway.

The time plot next to each cell or gate describes the dynamics of this circuit. In the case shown, the sharp increase and then decrease of the time plot at the lower right of figure 7 indicates that an external input stimulates the horizontal pathway. In response to the stronger signal being transmitted to the next level, the amount of transmitter in the gate inactivates, or habituates, during stimulation and then rises back toward the baseline level upon stimulus offset. Notice that the inactivation and reactivation of transmitter occur more slowly than changes in the activities of the neural cells. Each slowly habituating transmitter multiplies, or gates, the more rapidly varying signal in its pathway, thereby yielding net overshoots and undershoots at input onset and offset, respectively. During stimulation, the horizontal channel wins the rectified opponent competition against the vertical channel as indicated in the top-right time plot. However, upon offset of the stimulation to the horizontal channel, the input signal returns to the baseline level but the horizontal transmitter gate remains habituated below its baseline value. As a result, shortly after stimulus offset, the gated tonic input in the horizontal channel has a net signal *below the baseline level.* Meanwhile, the vertical pathway maintains the baseline response at all cells and gates before the opponent competition. Thus, when the horizontal channel is below the baseline activity, after stimulus offset, the vertical channel wins the rectified opponent competition and produces a rebound of activity as shown in the top-left time plot. As the horizontal transmitter gate recovers from its habituated state, the rebound signal in the vertical channel weakens and finally disappears. The duration of the transient rebound thus matches the recovery rate of the transmitter from habituation.

Figure 8 shows how this rebound of activity acts as a reset signal in the full BCS architecture. Figure 8a schematizes how inputs in a horizontal pathway excite a horizontal bipole cell. Through their positive feedback to hypercomplex cells, these horizontal bipole cells can generate hysteresis that produces persistence of the segmentation. Owing to the interactions of the gated-dipole circuit, offset of the horizontal input generates a rebound of activity in the vertical pathway, which, as figure 8b

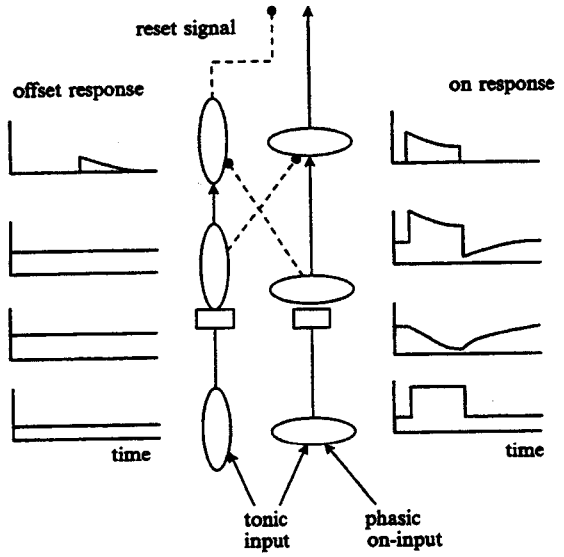

Figure 7. At stimulus offset, a gated dipole circuit produces a transient rebound of activity in the nonstimulated opponent pathway.

demonstrates, inhibits the horizontal bipole cell and decreases persistence. This reset property speeds the erosion of boundaries from contour ends to contour middle.

These properties of reset signals also explain why persistence of static stimuli varies inversely with stimulus luminance and duration (eg Bowen et al 1974), why the persistence of illusory contours is greater than that of luminance contours and differently affected by stimulus duration (Meyer and Ming 1988), and how orientation-specific adaptation can increase or decrease persistence (Meyer et al 1975). Details of these properties are in Francis et al (1994). In section 3 we show how the properties of the reset signals correspond to psychophysical measures of cortical afterimages.

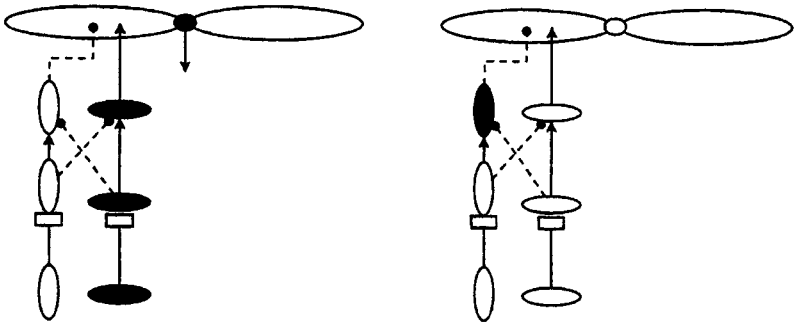

Figure 8. (a) A horizontal input excites a horizontal bipole cell that supports persistence. (b) Upon offset of the horizontal input, a rebound of activity in the vertical pathway inhibits the horizonal bipole cell. This inhibition resets the hysteresis of the feedback loop and reduces persistence.

3 Cortical afterimages

In the previous sections we reviewed mechanisms for boundary and brightness detection. Positive feedback in these mechanisms produce strong hysteresis, which requires additional mechanism to reset the systems. The gated-dipole circuit provides opponent signals at stimulus offset to reset the feedback loops activated during stimulus onset. The functional role of these signals is to reset persisting segmentation signals and prevent blurring and smearing of changing images.

However, since the reset signals are oriented signals (with local orientation opposite to that of the original stimulus boundaries), we must consider whether the reset signals can form a new boundary segmentation. In section 3.1, we show that new segmentations generated by reset signals can sometimes give rise to orientational afterimages.

3.1 *Orientational afterimages*

Figure 9 shows simulation results for a stimulus consisting of a series of concentric outline squares (bright lines on a dark background) presented for 2 (simulated) s (compare with the image in figure 1). Black pixel points indicate locally horizontal boundary signals, white pixel points indicate locally vertical boundary signals, and mid-gray pixel points indicate no strong response to either local orientation. Figure 9a shows the BCS response while the concentric squares are present. When the stimulus is present, the local and global orientations of the boundary signals match, so the system generates appropriately oriented boundary signals that outline the luminance increments of the squares. Such segmentations can interact with the FCS to bind color and brightness percepts within the regions defined by the segmentation contours.

Figure 9b shows the response of the system 250 simulated ms after the offset of the luminous outline squares. Reset signals of locally opposite orientation have replaced the boundary signals responsive to the stimulus edges. Significantly, along the middle of the display there are vertical (and horizontal) segmentations that respond to the vertical column (horizontal row) of locally vertical (horizontal) reset signals. Along these columns (or rows) the bipole cells can complete a segmentation to make a perceived cross shape. This segmentation is analogous to the orientational afterimages noted by MacKay (1957).

It is important to note that these segmentations do not bind corresponding brightness or color percepts. In section 2.1 we described how FCS brightness and color signals are not bound to mismatched BCS segmentations. In this case the brightness signals are organized in horizontal rows (vertical columns) while the afterimage segmentations signals are organized in vertical columns (horizontal rows). This mismatch means that the perceived afterimage may not include percepts of color and brightness, but should include perceived oriented segmentations. This prediction corresponds to percepts of the afterimage.

Because there is nothing to reset the segmentation generated by reset signals, the afterimage can persist for a substantial length of time. Figure 9c shows the system response 1.95 simulated s after the stimulus was turned off. The cross-shaped segmentation persists, even though the remaining reset signals weaken (closer to mid-gray).

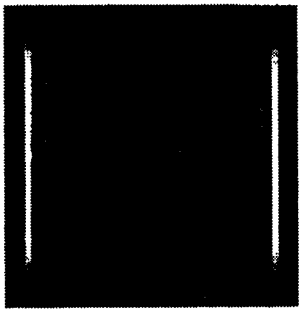

(a) time = 1150 ms

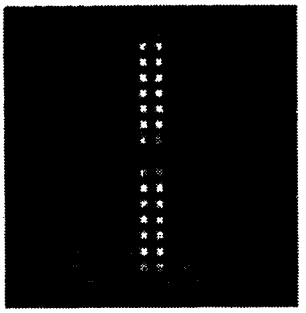

(b) time = 2250 ms

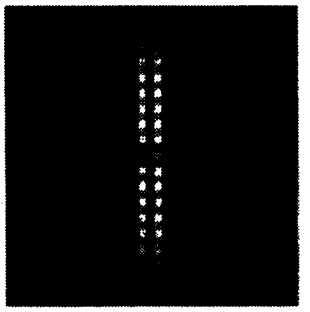

(c) time = 3950 ms

Figure 9. The spatial organization of segmentation and reset signals for a set of concentric outline squares. Gray level codes local orientations: black, horizontal; white, vertical; mid-gray, no local orientation. (a) While the stimulus is present, the boundary segmentation follows the luminance edges. Local orientations agree with global orientations. (b) After stimulus offset, reset signals appear. Along the center axes of the image, the local and global orientations match, thereby allowing the BCS to generate segmentations at those regions. These segmentations correspond to the perceived orientational afterimage, seconds. (c) Even as the reset signals fade away, the afterimage segmentation persists.

Interestingly, MacKay (1957), Taylor (1958), and Schwartz (1980) described hypothetical neural circuits that are similar to the gated dipole. In those circuits, habituation and competition generate local rebounds of activity in a fashion similar to the gated dipole described here. The BCS defines such mechanisms in a mathematically precise way, and also has the ability to segment or group local orientations through a global process of cooperative and competitive feedback. We suggest that it is the global feedback process that establishes the strong, lasting percept of the segmentation afterimage. Moreover, while MacKay (1957), Taylor (1958), and Schwartz (1980) hypothesized opponent mechanisms to explain how the afterimage formed, they did not explain why such a circuit exists. We suggest that the circuit exists to reset persisting segmentations in visual-feedback circuits.

3.2 *Residual traces*

If reset signals always produced new segmentations, they could undermine their functional purpose, because massive smearing would result from the afterimage segmentations. Fortunately, reset signals do not generally create new segmentations. Figure 10 shows simulation results of BCS responses to a 50 ms dark square on a bright background. Figure 10a shows the activity and local orientation of signals at each pixel just before the visual display returns to the background level. The system responds most vigorously along the vertical and horizontal luminous edges. Moreover, the local orientations match the global orientation of each edge: locally vertical boundary signals (white) align in a vertical column; locally horizontal boundary signals (black) align in a horizontal row.

Figure 10b shows the response of the system 400 simulated ms after stimulus offset. The only remaining signals are reset signals that have local orientations opposite to the original segmentation. Significantly, these reset signals do not generate a segmentation because their local orientation is perpendicular to their global organization. The reset signals along the horizontal edges of the stimulus are now locally vertical boundary signals (white), and the reset signals along the vertical edges of the stimulus are locally horizontal boundary signals (black). These signals inhibit, rather than excite, the horizontal and vertical bipole cells, respectively (see figure 8). As a result, the reset signals in this case do not generate a segmentation that can bind color and brightness of the original stimulus.

Figure 10 codes the *relative activities* of the BCS signals. The strength of reset signals in figure 10b are substantially smaller than the signals in figure 10a. If the reset signals are not too weak, they may be recognized by object-recognition pathways (see section 4), and referred to as a residual trace that has neither brightness, color, nor consistent orientation.

Thus, for this stimulus, the reset signals inhibit the persisting segmentation and do not generate a new segmentation. In this capacity, they efficiently prepare the system to build new segmentations without interference from past segmentations. Figure 2c demonstrates the effectiveness of the reset signals. This figure shows the simulated persistence of segmentation signals (see the appendix for details on the images and equations) over the range of luminances and durations used by Long and McCarthy (1982) with the same parameters as in Francis et al (1994). As stimulus duration or luminance increases, the persistence of the boundary signals decreases, in qualitative agreement with the data of Long and McCarthy shown in figure 2a. Figure 2e shows the same qualitative effects with an alternative choice of parameters to illustrate the robustness of the explanation of these data by the model.

We now show that the duration of these reset signals covaries with data on residual traces. The reset signals generated at stimulus offset are boundary signals of the locally orthogonal orientation, which observers may recognize through direct BCS

object-recognition pathways (see section 4). We hypothesize that subjects judging the duration of residual traces observe the strength of the reset signals. As was noted above to explain the inverse property for persistence of segmentations, the strength of reset signals increases with stimulus duration and luminance. Since the habituated gates in the gated dipole recover at a constant rate [see equation (A13) in the appendix], a stronger reset signal takes longer to passively fade away. Thus, reset-signal duration varies directly with stimulus duration and luminance, while the segmentations that they reset persist as an inverse function of stimulus duration and luminance. Figure 2d shows the duration of reset signals generated at stimulus offset. The duration of these signals increases as stimulus duration or stimulus luminance increases, in qualitative agreement with the data of Long and McCarthy (1982) shown in figure 2b. Figure 2f shows the same qualitative effects with the alternative choice of parameters to illustrate the robustness of the explanation of these data by the model.

Significantly, the model uses the same mechanisms to explain properties of orientational afterimages and residual traces. In each case, the afterimage is due to reset signals that exist to prevent massive smearing. Thus, the model explains *why* such afterimages exist in terms of mechanisms necessary to reduce visual persistence. The model hereby links orientational afterimages and residual traces to properties of visual persistence and a wide range of spatial properties of visual perception with a common model.

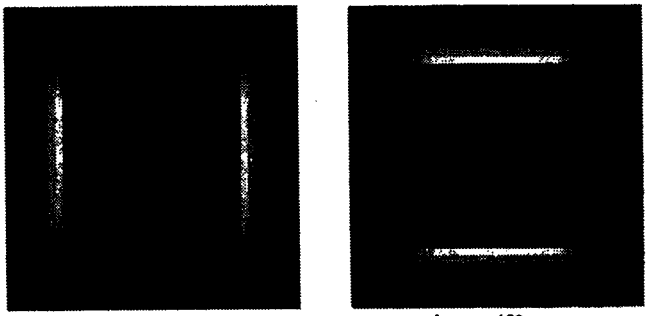

Figure 10. The spatial organization of segmentation and reset signals for a dark square on a bright background. Gray level codes local orientations: black, horizontal; white, vertical; mid-gray, no local orientation. (a) While the stimulus is present, the boundary segmentation outlines the luminance edges. Local orientations agree with global orientations. (b) Later, after boundary erosion, only reset signals remain. The local orientation of the reset signals is in conflict with the global organization of the signals, so the BCS cannot generate a segmentation.

3.3 *Residual traces in other paradigms*

While Long and McCarthy (1982) argued that residual traces measure persistence, critics of the study of residual traces have argued that they should not be considered measures of visual persistence. We agree with the critics on this point. Visual persistence is a measure of the original percept generated by the stimulus. Reset signals (and, we suggest, residual traces) are activations generated by the offset of the stimulus. The distinction is similar to that applied to retinal afterimages, which are clearly distinct from the original percept. Thus, while we feel residual traces should be studied in their own right, they should not be described as visual persistence.

These issues aside, we must consider why evidence of residual traces is not found in other measures of persistence. Studies of temporal integration divide a visual stimulus pattern into small parts and distribute those parts across two images. Subjects view the images in rapid succession (possibly separated by an interstimulus interval,

ISI) and perform a task that requires temporal integration of the displays. For example, Hogben and DiLollo (1974) used a display consisting of a 5×5 matrix and two frames of twelve dots each. The subject's task was to report the location of the missing dot among the two frames. As the ISI increased, the task became more difficult and the number of correct identifications decreased. The percentage correct gives an indication of the persistence of the elements from the leading display. Since the subject must identify the missing element by using whatever information is available, one might expect that subjects would attend to residual traces to perform the task. Psychophysical studies, however, indicate that as stimulus luminance or duration increases, performance worsens, indicating shorter persistence of the elements, and indicating that subjects cannot use residual traces (if they exist).

The model explains why integration (and other) studies do not reveal the properties of residual traces. Since residual traces are reset signals that usually cannot form a new segmentation, they are usually uninformative for the integration tasks. As a result, subjects are forced to rely upon integration of perceived brightness in the FCS. Since reset signals cannot bind FCS signals, their presence is not revealed in those studies.

Figure 11 schematizes how the model accounts for these findings. Figure 11a shows the stimulus configuration and the resulting BCS and FCS signals produced by the model under conditions of a short ISI, which is likely to allow integration. Note that in

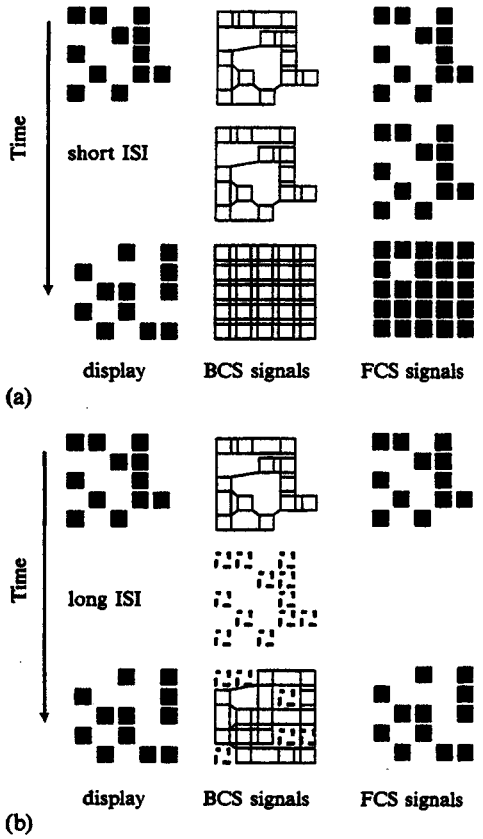

Figure 11. Schematic of the response of the model to an integration display where the subject must identify the location of the missing element from the two frames. (a) For short ISIs, the BCS signals are uninformative because of interelement boundaries, while the FCS signals allow easy identification. (b) For long ISIs, the BCS signals are again uninformative (despite long-lasting reset signals coded as dashed lines) and FCS signals are also uninformative.

addition to the stimulus boundaries, the BCS generates boundaries between elements that correspond to perceived groupings of elements (Grossberg and Mingolla 1985b). These grouping boundaries coexist with the boundaries generated by luminance edges, but do not produce percepts of brightness because no FCS signals exist to be bound by the boundaries. With a short ISI, the BCS signals from the first frame persist and integrate with BCS signals generated by the onset of the second frame. Boundaries are thereby created between elements from both frames, rendering BCS signals uninformative about the location of the missing element. On the other hand, the FCS uniquely identifies the location of the missing element because no FCS signal exists at that location.

Figure 11b schematizes BCS and FCS signals under conditions of a long ISI. During the ISI BCS signals generated by the leading frame erode away and are replaced by orientationally opposite reset signals. These reset signals are unable to bind FCS activities. After onset of the second display, the reset signals coexist with boundaries generated by the elements of the second display. However, grouping boundaries between elements of the second frame 'write over' some of the reset signals from the first display, and possibly over the empty space of the missing element. Thus, the BCS signals are generally uninformative about the location of the missing element. The FCS signals are also uninformative in this display because no FCS signals from the first frame persist to integrate with the FCS signals from the second frame.

In general, in a temporal-integration display subjects must integrate brightness percepts to perform the task, and FCS signals coding brightness do not reveal the presence of reset signals (residual traces). Thus, the model predicts that any task that depends on judging offset of the brightness percept will not reveal evidence of residual traces. Judgments of perceived brightness offset are, we suspect, the norm in studies of visual persistence.

However, the model suggests a way of investigating residual traces with integration studies. Since the bipole cells require inputs on both sides of their receptive fields to generate grouping boundaries, when the missing element is located at one of the four corners of the matrix, no residual traces or grouping boundaries should be produced in that location. All other matrix elements should have either residual traces or stimulus boundaries. Thus, with practice, subjects may be able to use the presence of residual traces to help identify the location of the missing element.

4 Seeing vs recognizing

It remains to say how BCS reset signals can be detected by an observer even if they do not bind FCS brightness or color signals. Given that BCS output signals are insensitive to contrast polarity, they do not carry their own visible signals. What kind of detection, then, can a BCS signal generate in the absence of FCS support?

The answer to this question depends upon how FACADE theory explains the difference between seeing and recognizing (Grossberg 1987a, 1994). For purposes of recognition, BCS signals input directly to the Object-Recognition System (ORS), thereby allowing recognition of boundary signals without requiring corresponding brightness or color percepts. The FCS can also directly input to the ORS, thereby facilitating recognition due to surface qualities such as brightness, color, and depth. Grossberg (1994) summarized experimental evidence for BCS and FCS processing in the interblob-processing and blob-processing streams of the visual cortex, respectively, and for the ORS in the temporal cortex.

Figure 12 schematizes this global architecture. The distinction between seeing, which occurs in the FCS, and recognizing, which occurs in the ORS owing to either FCS or BCS signals, is critical to understanding the properties of residual traces and

orientational aftereffects. This distinction has a long history in visual perception, in modified form, as the distinction between seeing and thinking, or the related distinction between modal and amodal perception (Epstein 1993; Gregory 1993; Kanizsa 1979; Kellman and Shipley 1991; Michotte et al 1964). Properties of the BCS, FCS, and ORS help to resolve controversies that still persist based on these classical concepts. For example, the BCS explicates why *all* boundary segmentations are perceptually invisible, or amodal, owing to the fact that BCS output signals are insensitive to contrast polarity. These invisible segmentations can nonetheless generate large activations of ORS recognition codes, so one can 'know' about a segmentation that one cannot 'see'. The FCS can generate visible surface representations because its output signals are sensitive to contrast polarity. The theory predicts that, when we see a boundary, it is because there is a discontinuity in filled-in surface qualities like brightness or color within the FCS due to signals from the BCS that prevent filling in across the intervening boundary. Thus the BCS supports perception of visible, or modal, boundaries in the FCS, but is not itself a substrate of visible representations. BCS $\rightarrow$ ORS signals permit detection of a residual trace or afterimage even if it is not supported by discontinuities in the filled-in FCS surface representation. In other words, a residual trace can be amodally registered by a 'cognitive' process of object recognition even if it is not modally seen as a surface-brightness difference. Furthermore, some residual traces can be amodally recognized even if they do not generate long-term afterimages.

The model distinction between amodal recognition of residual traces via BCS $\leftrightarrow$ ORS interactions and modal perception of persistence via BCS $\leftrightarrow$ FCS interactions may help to clarify the difference between visible persistence, whose duration varies inversely with stimulus intensity, and subsequent nonvisible processes, whose duration may vary directly with intensity. Various authors have posited such a nonvisible process to decode the information in a display, whether as a 'nonvisible trace' (Sperling 1967), a 'nonvisible identity code' (Irwin and Yeomans 1986b), or as 'informational persistence' (Coltheart 1980). See DiLillo and Bischof (1995) for an excellent review. From the present account it is suggested that there also exists a nonvisible trace whose duration varies directly with intensity and that is amodally recognized but that, in itself, does not play a role in processing the information in the visible trace.

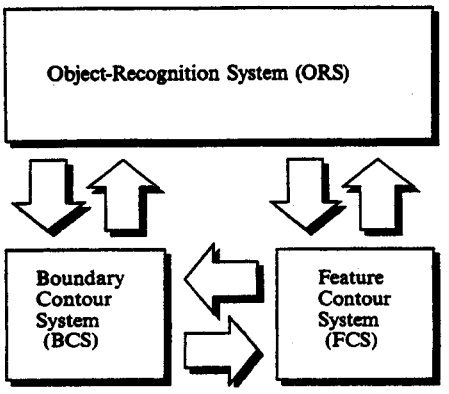

Figure 12. Signals in the FCS correspond to percepts of surface brightness, color, and depth. Boundary segmentation signals in the BCS control the FCS percepts. An Object-Recognition System (ORS) can recognize the spatial layout of oriented BCS signals even if no associated brightness or color percepts are generated in the FCS.

5 Conclusions

The FACADE model conceptually links disparate data on the spatial and dynamic properties of visual processing at stimulus offset. We have shown that the dynamic properties of reset signals may be used to explain and clarify evidence of cortical afterimages. It is suggested from figures 9 and 10 that the main qualitative difference between the orientational afterimages studied by MacKay (1957) and the residual traces studied by Long and McCarthy (1982) is the spatial organization of the reset signals generated at stimulus offset. According to the model, when the reset signals have a spatial structure that can produce a segmentation, subjects should perceive an orientational afterimage, which in the current simulations cannot bind color and brightness percepts. On the other hand, when the reset signals have a spatial structure that cannot produce a segmentation, subjects should recognize the reset signals as a residual trace produced by the stimulus offset, but should not perceive a coherent segmentation that binds color and brightness.

In all these simulations, our intention has been to show how the qualitative properties of the model conceptually clarify diverse data sets, rather than to produce a precise quantitative fit to any one piece of the data. Indeed, the model simplifications (eg only two orientations) necessary to make the computations feasible make a search for optimal parameters premature. As noted in Francis et al (1994), the model properties are robust across a wide range of parameter choices.

The model links these apparently disparate sets of data with additional data on the persistence of segmentations (Francis 1996a; Francis et al 1994), temporal integration (Francis 1996b), and metacontrast masking (Francis 1995). The simulation characteristics used to explain the dynamic processing of visual images remain consistent with, and depend upon, the previous explanations, by the theory, of illusory contours (Grossberg and Mingolla 1985a), texture segregation (Grossberg and Mingolla 1985b), shape from shading (Grossberg and Mingolla 1987), 3-D vision (Grossberg 1987b, 1993, 1994), and motion processing (Francis and Grossberg 1996; Grossberg 1991), among others. The unifying conceptual links between these data sets that are provided by the model have already begun to suggest fertile new lines of experimental inquiry.

Acknowledgements. The authors wish to thank Diana Meyers and Robin Locke for their valuable assistance in the preparation of the manuscript. Stephen Grossberg was partially supported by the Air Force Office of Scientific Research (ASOSR F49620-92-J-0499), the Advanced Research Projects Agency (ONR N00014-92-J-4015), and the Office of Naval Research (ONR N00014-91-J-4100).

References

Bowen R, Pola J, Matin L, 1974 "Visual persistence: Effects of flash luminance, duration and energy" *Vision Research* **14** 295–303

Brown J, 1965 "Afterimages", in *Vision and Visual Perception* Ed. C H Graham (New York: John Wiley) pp 479–503

Castet E, 1994 "Effect of the ISI on the visible persistence of a stimulus in apparent motion" *Vision Research* **34** 2103–2144

Cavanagh P, Arguin M, Grünau M von, 1989 "Interattribute apparent motion" *Vision Research* **29** 1197–1204

Cohen M A, Grossberg S, 1984 "Neural dynamics of brightness perception: Features, boundaries, diffusion, and resonance" *Perception & Psychophysics* **36** 428–456

Coltheart M, 1980 "Iconic memory and visible persistence" *Perception & Psychophysics* **27** 183–228

DiLollo V, 1984 "On the relationship between stimulus intensity and duration of visible persistence" *Journal of Experimental Psychology: Human Perception and Performance* **10** 754–769

DiLollo V, Bischof W, 1995 "The inverse-intensity effect in duration of visible persistence" *Psychological Bulletin* **118** 223–237

DiLollo V, Clark C, Hogben J, 1988 "Separating visible persistence from retinal afterimages" *Perception & Psychophysics* **44** 363–368

Epstein W, 1993 "On seeing that thinking is separate and on thinking that seeing is the same" *Italian Journal of Psychology* **20** 731–747

Farrell J, Pavel M, Sperling G, 1990 "The visible persistence of stimuli in stroboscopic motion" *Vision Research* **30** 921–936

Francis G, 1995 "Cortical dynamics of lateral inhibition: Metacontrast masking" technical report 95-2, Purdue Mathematical Psychology Program, West Lafayette, IN (submitted for publication)

Francis G, 1996a "Cortical dynamics of lateral inhibition: Visual persistence and ISI" *Perception & Psychophysics* in press

Francis G, 1996b "Cortical dynamics of visual persistence and temporal integration" *Perception & Psychophysics* in press

Francis G, Grossberg S, 1996 "Cortical dynamics of form and motion integration: Persistence, apparent motion, and illusory contours" *Vision Research* **36** 149–174

Francis G, Grossberg S, Mingolla E, 1994 "Cortical dynamics of binding and reset: Control of visual persistence" *Vision Research* **34** 1089–1104

Gove A N, Grossberg S, Mingolla E, 1994 "A link between brightness perception, illusory contours, and binocular corticogeniculate feedback" *Investigate Ophthalmology and Visual Science* **35** 1437

Gove A N, Grossberg S, Mingolla E, 1995 "Brightness perception, illusory contours, and corticogeniculate feedback" *Visual Neuroscience* **12** 1027–1052

Gregory R L, 1993 "Seeing and thinking" *Italian Journal of Psychology* **20** 749–769

Grossberg S, 1972 "A neural theory of punishment and avoidance: II. Quantitative theory" *Mathematical Biosciences* **15** 253–285

Grossberg S, 1983 "The quantized geometry of visual space: The coherent computation of depth, form, and lightness" *Behavioral and Brain Sciences* **6** 625–657

Grossberg S, 1984 "Outline of a theory of brightness, color, and form perception", in *Trends in Mathematical Psychology* Eds E Degreef, J van Buggenhaut (Amsterdam: Elsevier/North-Holland) pp 59–86

Grossberg S, 1987a "Cortical dynamics of three-dimensional form, color, and brightness perception I: Monocular theory" *Perception & Psychophysics* **41** 97–116

Grossberg S, 1987b "Cortical dynamics of three-dimensional form, color, and brightness perception II: Binocular theory" *Perception & Psychophysics* **41** 117–158

Grossberg S, 1991 "Why do parallel cortical systems exist for the perception of static form and moving form?" *Perception & Psychophysics* **49** 117–141

Grossberg S, 1993 "A solution of the figure–ground problem for biological vision" *Neural Networks* **6** 463–484

Grossberg S, 1994 "3-D vision and figure–ground separation by visual cortex" *Perception & Psychophysics* **55** 48–120

Grossberg S, Mingolla E, 1985a "Neural dynamics of form perception: Boundary completion, illusory figures, and neon color spreading" *Psychological Review* **92** 173–211

Grossberg S, Mingolla E, 1985b "Neural dynamics of perceptual grouping: Textures, boundaries, and emergent segmentations" *Perception & Psychophysics* **38** 141–171

Grossberg S, Mingolla E, 1987 "Neural dynamics of surface perception: Boundary webs, illuminants, and shape-from-shading" *Computer Vision, Graphics, and Image Processing* **37** 116–165

Grossberg S, Mingolla E, Todorović D, 1989 "A neural network architecture for preattentive vision" *IEEE Transactions on Biomedical Engineering* **36** 65–84

Grossberg S, Mingolla E, Williamson J, 1994 "Synthetic aperture radar processing by a multiple scale neural system for boundary and surface representation" technical report CAS/CNS-TR-94-001, Boston University, Boston, MA

Grossberg S, Todorović D, 1988 "Neural dynamics of 1-D and 2-D brightness perception: A unified model of classical and recent phenomena" *Perception & Psychophysics* **43** 241–277

Grossberg S, Wyse L, 1991 "Invariant recognition of cluttered scenes by a self-organizing ART architecture: Figure–ground separation" *Neural Networks* **4** 723–742

Grünau M von, 1979 "The involvement of illusory contours in stroboscopic motion" *Perception & Psychophysics* **25** 205–208

Hawkins H, Shulman G, 1979 "Two definitions of persistence in visual perception" *Perception & Psychophysics* **25** 348–350

Heydt R von der, Peterhans E, Baumgartner G, 1984 "Illusory contours and cortical neuron responses" *Science* **244** 1260–1262

Hogben J, DiLollo V, 1974 "Perceptual integration and perceptual segregation of brief visual stimuli" *Vision Research* **14** 1059–1069

Irwin D E, Yeomans J M, 1986a "Persisting arguments about visual persistence: Reply to Long" *Perception & Psychophysics* **39** 225–230

Irwin D E, Yeomans J M, 1986b "Sensory registration and informational persistence" *Journal of Experimental Psychology: Human Perception and Performance* **12** 343–360

Kanizsa G, 1979 *Organization in Vision* (New York: Praeger)

Kaufman L, 1974 *Sight and Mind* (Oxford: Pergamon Press)

Kellman P J, Shipley T F, 1991 "A theory of visual interpolation in object perception" *Cognitive Psychology* **23** 141–221

Kolers P, 1972 *Aspects of Motion Perception* (New York: Oxford University Press)

Korte A, 1915 "Kinematoskopische Untersuchungen" *Zeitschrift für Psychologie* 194–296

Long G, 1980 "Iconic memory: A review and critique of the study of short-term visual storage" *Psychological Bulletin* **88** 785–820

Long G, McCarthy P, 1982 "Target energy effects on Type I and Type II visual persistence" *Bulletin of the Psychonomic Society* **19** 219–221

Long G, Sakitt B, 1981 "Differences between flicker and non-flicker persistence tasks: The effects of luminance and the number of cycles in a grating target" *Vision Research* **21** 1387–1393

Long G, Wurst S, 1984 "Complexity effects on reaction-time measures of visual persistence: Evidence for peripheral and central contributions" *American Journal of Psychology* **4** 537–561

Ludtke D, 1992 *NXPlot3D Version 3.0* Physics Department, Rice University, Houston, TX

MacKay D, 1957 "Moving visual images produced by regular stationary patterns" *Nature (London)* **180** 849–850

McFarland J, 1965 "Sequential part presentation: A method of studying visual form perception" *British Journal of Psychology* **56** 439–446

Meyer G, Ming C, 1988 "The visible persistence of illusory contours" *Canadian Journal of Psychology* **42** 479–488

Meyer G, Lawson R, Cohen W, 1975 "The effects of orientation-specific adaptation on the duration of short-term visual storage" *Vision Research* **15** 569–572

Michotte A, Thines G, Crabbe G, 1964 *Les complements amodaux des structures perceptives* (Louvain: Publications Universitaires)

Neuhaus W, 1930 "Experimentalle Untersuchung der Scheinbewegung" *Archiv für die Gesamte Psychologie* **75** 315–458

Pessoa L, Mingolla E, Neumann H, 1995 "A contrast- and luminescence-driven multiscale network model of brightness perception" *Vision Research* **35** 2201–2223

Schwartz E, 1980 "Computational anatomy and functional architecture of striate cortex: A spatial mapping approach to perceptual coding" *Vision Research* **20** 645–669

Sperling G, 1967 "Successive approximations to a model for short-term memory" *Acta Psychologica* **27** 285–292

Taylor W, 1958 "Visual organization" *Nature (London)* **182** 29–31

APPENDIX

The network equations and parameters are identical to those used in Francis et al (1994). They are reprinted here to make the present paper self-contained.

A.1 Network equations

Level 0: Image plane

Each pixel has a value associated with retinal luminance. We describe the pixel-luminance values of the different stimuli used in the simulations below.

Level 1: Center–surround cells

The activity X_{ij}^1 of a level-1 cell centered at position (i, j) obeys a shunting on-center, off-surround equation

$$\frac{dX_{ij}^1}{dt} = -X_{ij}^1 + (A - X_{ij}^1)\sum_{pq} B_{ijpq} I_{pq} - (X_{ij}^1 + C)\sum_{pq} D_{ijpq} I_{pq}, \tag{A1}$$

where I_{pq} is the retinal luminance at position (p, q), A is the maximum activity of the cell, $-C$ is the minimum activity of the cell, and

$$B_{ijpq} = B\exp\{-\alpha^{-2}\log 2[(i-p)^2 + (j-q)^2]\}, \tag{A2}$$

$$D_{ijpq} = D\exp\{-\beta^{-2}\log 2[(i-p)^2 + (j-q)^2]\} \tag{A3}$$

are excitatory and inhibitory Gaussian weighting functions, respectively. The term $\log 2$ means the parameters α and β set the radius of their respective Gaussians at half strength. Parameters B and D are constant scaling terms.

To save computation, the equilibrium response of the differential equation is found by setting the left-hand side of equation (A1) equal to zero. The resulting algebraic equation can be solved to find

$$X_{ij}^1 = \frac{A\sum_{pq} B_{ijpq} I_{pq} - C\sum_{pq} D_{ijpq} I_{pq}}{1.0 + \sum_{pq}(B_{ijpq} + D_{ijpq}) I_{pq}}. \tag{A4}$$

The activities of cells at this level share some key properties with those found in ganglion cells or LGN (Grossberg and Torodorić 1988). No off-center on-surround cells were implemented in our simulations.

Level 2: Oriented simple cells

The following equations define oriented simple cells that are centered at position (i, j) with preferred orientation k. To create a vertically oriented input field, or in-field, that is specific to the polarity of the luminance gradient, divide an elongated region into a left half L_{ijk} and a right half R_{ijk}. Add up the weighted sum of the level-1 inputs within the range of the left side

$$F_{ijk} = \sum_{pq \in L_{ijk}} E_{ijpq} X_{pq}^1 \tag{A5}$$

and the right side

$$G_{ijk} = \sum_{pq \in R_{ijk}} E_{ijpq} X_{pq}^1 \tag{A6}$$

of the region, with

$$E_{ijpq} = \exp[-\gamma^{-2}\log 2(i-p)^2] \tag{A7}$$

decreasing for inputs further away from the oriented center line of the in-field; the parameter γ controls the rate of fall off. Then a simple cell that is selectively responsive to a bright-to-dark luminance gradient obeys the differential equation

$$\frac{dX_{ijk}^{2BD}}{dt} = -X_{ijk}^{2BD} + [F_{ijk} - G_{ijk}]^+, \tag{A8}$$

where $[p]^+ = \max(p, 0)$. A cell responsive to a dark-to-bright luminance gradient obeys the equation

$$\frac{dX_{ijk}^{2DB}}{dt} = -X_{ijk}^{2DB} + [G_{ijk} - F_{ijk}]^+. \tag{A9}$$

To save computation, the activities of these cells were computed at equilibrium as

$$X_{ijk}^{2BD} = [F_{ijk} - G_{ijk}]^+ \tag{A10}$$

and

$$X_{ijk}^{2DB} = [G_{ijk} - F_{ijk}]^+. \tag{A11}$$

Level 3: Oriented complex cells

Each cell in level 3 becomes insensitive to the polarity of contrast by summing the rectified activities of the cells in level 2 of the same location and orientation. Each level-3 cell obeys the differential equation

$$\frac{dX_{ijk}^{3}}{dt} = -X_{ijk}^{3} + H(X_{ijk}^{2BD} + X_{ijk}^{2DB}). \tag{A12}$$

Parameter H scales the activities of the input signals to the complex cell.

Level 4: Habituative transmitter gates

The signal in each oriented pathway is gated, or multiplied, by a habituative transmitter which obeys the equation (Grossberg, 1972)

$$\frac{dX_{ijk}^{4}}{dt} = K[L(M - X_{ijk}^{4}) - (X_{ijk}^{3} + J)X_{ijk}^{4}]. \tag{A13}$$

This equation indicates that the amount of available transmitter X_{ijk}^4 accumulates to the level M, via term $KL(M - X_{ijk}^4)$, and is inactivated by mass action at rate $K(X_{ijk}^3 + J)X_{ijk}^4$, where J is the tonic input of a gated dipole and X_{ijk}^3 is its phasic increment. We set the rate K much smaller than 1.0 so that these equations operate on a slower time scale than the equations describing cell activities. At the beginning of each simulation, each transmitter value is set to the nonstimulated equilbrium value $X_{ijk}^4 = LM/(L + J)$.

Level 5: First competitive stage of hypercomplex cells

The gated signals of a fixed orientation compete via on-center off-surround spatial interactions. Along with the tonic signal coming up through the habituative transmitters, each cell also receives a tonic input which supports disinhibitory activations at the next competitive stage (see Grossberg and Mingolla 1985a, 1985b). The activity of a level-5 cell obeys the differential equation

$$\frac{dX_{ijk}^{5}}{dt} = -X_{ijk}^{5} + J + (X_{ijk}^{3} + J)X_{ijk}^{4} + NX_{ijk}^{8} - X_{ijk}^{5}\sum_{pq} P_{ijpq}(X_{pqk}^{3} + J)X_{pqk}^{4}, \tag{A14}$$

where $-X_{ijk}^5$ models passive decay, the parameter J establishes a nonzero baseline of activity for the cell, the term $(X_{ijk}^3 + J)X_{ijk}^4$ is the gated excitatory input from the lower level at the same position and orientation, the term NX_{ijk}^8 is a feedback signal

from the higher-level cell of the same position and orientation, and the term $X^5_{ijk}\sum_{pq}P_{ijpq}(X^3_{pqk}+J)X^4_{pqk}$ is the inhibitory input from the lower-level cells of the same orientation and nearby spatial positions. The inhibitory weights fall off in strength as the spatial distance between cells increases, as in

$$P_{ijpq}=P\exp\{-\delta^{-2}\log 2[(i-p)^2+(j-q)^2]\}, \tag{A15}$$

where P scales the strength of the inhibition, and δ controls the spread.

For the simulations in this paper, the differential equation was solved at equilibrium as

$$X^5_{ijk}=\frac{J+(X^3_{ijk}+J)X^4_{ijk}+NX^8_{ijk}}{1.0+\sum_{pq}P_{ijpq}(X^3_{pqk}+J)X^4_{pqk}}. \tag{A16}$$

Level 6: Second competitive stage of hypercomplex cells
The output signals from the first competitive stage compete across orientation at each position. The activity of a cell receiving this competition obeys the differential equation

$$\frac{dX^6_{ijk}}{dt}=-X^6_{ijk}+(X^5_{ijk}-X^5_{ijK}), \tag{A17}$$

where X^5_{ijk} and X^5_{ijK} represent orthogonal orientations.

Level 7: Cooperative bipole cells and spatial impenetrability
The next level involves a simplified version of bipole cells. As in level 1, we divide the in-field of each horizontal bipole cell into a left side L_{ijk} and a right side R_{ijk} (top and bottom for vertically oriented bipole cells). Each bipole cell then sums up excitatory like-oriented signals and inhibitory orthogonally oriented signals within each side. A slower-than-linear bounded function squashes the net signal of each side. We then set the output threshold of the bipole cells so that boundaries must stimulate both sides of the receptive field for the cell to generate an output signal. The differential equation describing each bipole cell activity is

$$\frac{dX^7_{ijk}}{dt}=X^7_{ijk}+f\left(\sum_{pq\in R_{ijk}}[X^6_{pqk}]^+-[X^6_{pqK}]^+\right)+f\left(\sum_{pq\in L_{ijk}}[X^6_{pqk}]^+-[X^6_{pqK}]^+\right), \tag{A18}$$

where

$$f(w)=\frac{Qw}{1.0+w} \tag{A19}$$

acts to squash the net input on each side of the receptive field of the bipole cell so that it never exceeds the value of parameter Q. Grossberg and Mingolla (1985b) use a more complicated bipole cell. Their bipole cells receive excitatory inputs from a range of orientations that are weighted by a function that decreases with spatial difference from (i, j) and orientational difference from k. Grossberg and Mingolla use these features to explain a variety of grouping phenomena, but simpler bipole cells suffice to simulate the basic properties of boundary signal persistence.

Level 8: Spatial sharpening
Output signals from the bipole cells are thresholded to prevent feedback unless inputs activate both sides. These output signals then undergo a spatial sharpening much as in the first competitive stage of level 5. The activities of cells in level 8 obey the differential equation

$$\frac{dX^8_{ijk}}{dt}=-X^8_{ijk}+[X^7_{ijk}-R]^+-X^8_{ijk}\sum_{pq\in S_{ij}}T[X^7_{pqk}-R]^+, \tag{A20}$$

where parameter R is the output threshold for bipole cells, parameter T scales the strength of the spatial inhibition, and S_{ij} is the eight nearest neighbors to pixel (i, j). These signals are scaled by parameter N before feeding back to the cells in level 5 to close the feedback loop.

A.2 Stimuli and parameters

In this section we describe the stimuli and measures used in the simulations. The equations and parameters for the simulations are the same as in Francis et al (1994), except as described below. The Francis et al (1994) parameters are: $A = 67.5$, $B = 2.5$, $C = 60.0$, $D = 0.05$, $H = 0.1$, $J = 20.0$, $K = 0.0003$, $L = 3.0$, $M = 5.0$, $N = 13.0$, $P = 0.0005$, $Q = 0.5$, $R = 0.61$, $T = 0.3$, $\alpha = 0.5$, $\beta = 3.0$, $\gamma = 1.5$, $\delta = 3.0$. Each side, L_{ijk} and R_{ijk}, of the oriented masks in level 2 were rectangles of 4 pixels $\times$ 1 pixel in size. Each side of a bipole cell was restricted to a single column (vertical) or row (horizontal) extending 18 pixels from the position of the bipole cell.

For all stimuli, dark means 0.000001 simulated ft L. The stimuli for the simulation results shown in figures 2c and 2d consisted of dark squares (26 pixels $\times$ 26 pixels) on a bright background (5.0 or 15.0 simulated ft L). These stimuli cover the range of luminances and durations used by Long and McCarthy (1982). Persistence of segmentation offset was measured by noting the time beyond stimulus offset when all the segmentation signals (activities in level 6) matching the local orientations produced during stimulus presentation dropped below a constant threshold value of 0.05 units. Duration of reset signals (residual traces) was measured by noting the time beyond stimulus offset when all the reset signals (level-6 activities with local orientations opposite to those produced during stimulus presentation) dropped below the same threshold value. For the simulations summarized in figures 2e and 2f, the threshold value was 0.09 instead of 0.05, and the following parameter changes were made: $B = 0.5$, $D = 0.01$, and $K = 0.003$; all other parameters remained the same.

The simulations that produced figures 9 and 10 differed slightly from the simulations described in Francis et al (1994) and the other simulations reported here. In these simulations, each boundary signal sent to a bipole cell of the opposite orientation is multiplied by the value 10 [see equation (A18)]. This weighting describes the strength of spatial impenetrability, which prevents the creation of spurious segmentations (Grossberg and Mingolla 1985b). This property was not relevant in previous studies, but it is here. Such a parameter change in no way modifies the qualitative properties of the simulation results reported in Francis et al (1994) or in the other simulations reported here, although the quantitative values produced would differ. Since the model is now at the stage of explaining large bodies of qualitative data properties, no loss is caused by this parameter change.

The stimulus for figure 10 was a dark square (26 pixels $\times$ 26 pixels) on a bright (2.0 ft L) background present for 50 simulated ms. The stimulus for figure 9 was a series of four concentric, bright (0.25 simulated ft L) outline squares, 1 pixel wide each, separated by 3 pixels of dark background present for 2 simulated s. [Note: 1 ft L = 3.43 cd m^{-2}.]

All equations were solved by using Euler's method with a step size of 0.01 time units. Cell activities were checked every 0.1 time units (1 simulated ms) to measure persistence of the signals. All simulations were performed on a Silicon Graphics Indy R4000 SC workstation. The data in figures 9 and 10 were generated with the graphing program NXPlot3D (Ludtke 1992).